Supporting Information

Nickel Doped Iron Oxide Nanoparticles Conjugated Porphyrin Interface (Porphyrin/Fe_2O_3@Ni) for Non-enzymatic Detection of Dopamine from Lacrimal Fluid

Umay Amara,[1,2] Khalid Mahmood,[*2] Muhammad Awais,[2] Muhammad Khalid,[3] Muhammad Nasir,[1] Sara Riaz,[4] Akhtar Hayat,[1] Mian Hasnain Nawaz[*1]

[1]Interdisciplinary Research Centre in Biomedical Materials (IRCBM), COMSATS University Islamabad, Lahore Campus 54000, Pakistan

[2]Institute of Chemical Sciences, Bahauddin Zakariya University, Multan 60800, Pakistan

[3]Department of Basic Sciences & Humanities, Khwaja Fareed University of Engineering & Information Technology, Rahim Yar Khan 64200, Pakistan
[4] Department of Chemistry, COMSATS University Islamabad, Lahore Campus 54000, Pakistan

Correspondence: (K.M.) khalidmahmood@bzu.edu.pk ; (M.H.N.) mhnawaz@cuilahore.edu.pk

1. Experimental Section

1.1 Chemicals and reagents

Porphyrin i.e. 5,10,15,20-(Tetra-4-carboxyphenyl), Iron chloride ($FeCl_3 \cdot 6H_2O$, 99.8%), Nickel nitrate hexahydrate ($Ni(NO_3)_3$.6H2O), dopamine (DA), glucose (Glu), fructose, L-Cysteine, urea, uric acid (UA), potassium ferrocyanide ($K_4Fe(CN)_6$), phosphate buffer saline (PBS) and potassium ferricyanide ($K_3Fe(CN)_6$) and ascorbic acid (AA), were brought from Sigma-Aldrich Ltd. All the chemicals were of analytical grades and utilized without further purification.

1.2 Characterization Techniques

X-ray diffraction (XRD) graphs were obtained by utilizing Rigaku D/max-2550 instrument with a Cu-Kα radiation source (λ=1.5418 Å) to investigate the phase composition. Scanning electron microscopy was executed to examine surface morphologies were via TESCAN VEGA 3 for SEM analysis. Renishaw in Via-reflex spectrometer was used to record Raman spectra. For electrochemical analysis Gamry 1010 interface electrochemical analyzer was used. All the experiments were conducted at room temperature with a three-electrode system comprising GPE as working, platinum-based counter electrode and Ag/AgCl/Sat. KCl electrode as a reference electrode with a standard potential of (E=+0.197 V saturated). Meanwhile, the Electrochemical Impedance Spectroscopy (EIS) studies were conducted in the 5 mM ferro/ferri solution (1:1).

1.3 Real sample analysis Sample Preparation

To assess the practical application of the designed sensing interface, spiked human lacrimal fluid samples were assessed against DA. The serum was obtained from female volunteer in eppendorf and has been stored at 4 ^{o}C before use. Primarily, the obtained Human lacrimal fluid (500 µL) was diluted with (500 µL) of PBS pH (7.4). To obtain the desired analyte concentrations, the stock solution was prepared by shaking 5 mM DA solution (1000 µL) + diluted human lacrimal fluid solution (1000 µL). The recovery experiments were performed by adding aliquots from the freshly prepared stock solution.

The contents of the solutions are listed below.

40 µM= (160 µL aliquot from stock + 20 mL PBS)

75 µM= (300 µL aliquot from stock + 20 mL PBS)

100 µM= (400 µL aliquot from stock + 20 mL PBS)

500 µM= (2000 µL aliquot from stock + 20 mL PBS)

Finally, for analysis CV was performed on Porphyrin/Fe_2O_3@Ni based sensor at 0.20 V by adding aliquots after every 50 seconds.

$$Recovery\ \% = 100 - Relative\ Error \qquad (S1)$$

2 Results and Discussion

2.1 Limit of detection (LOD)

The limit of detection (LOD) was premeditated using equation S2.

$$\mathbf{LOD = F\ x\ SD/}\boldsymbol{b} \qquad \mathbf{(S2)}$$

Wherein,

F is the factor of 3.3, SD is the standard deviation of blank sample, and b is the slope of regression line.

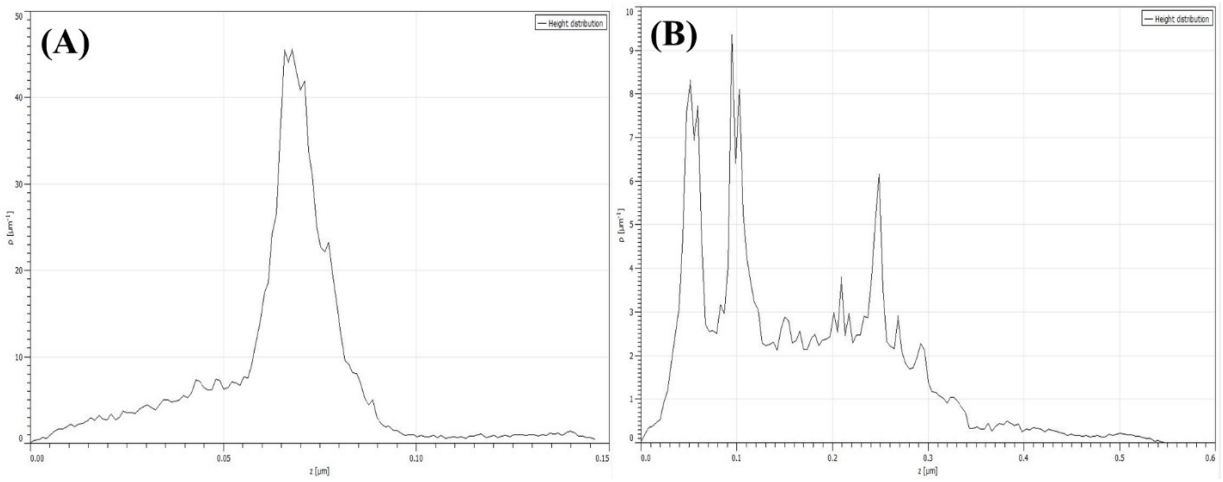

Fig. S1. Surface height distribution of (A) Fe_2O_3@Ni (B) Porphyrin/ Fe_2O_3@Ni obtained via atomic force microscopy.

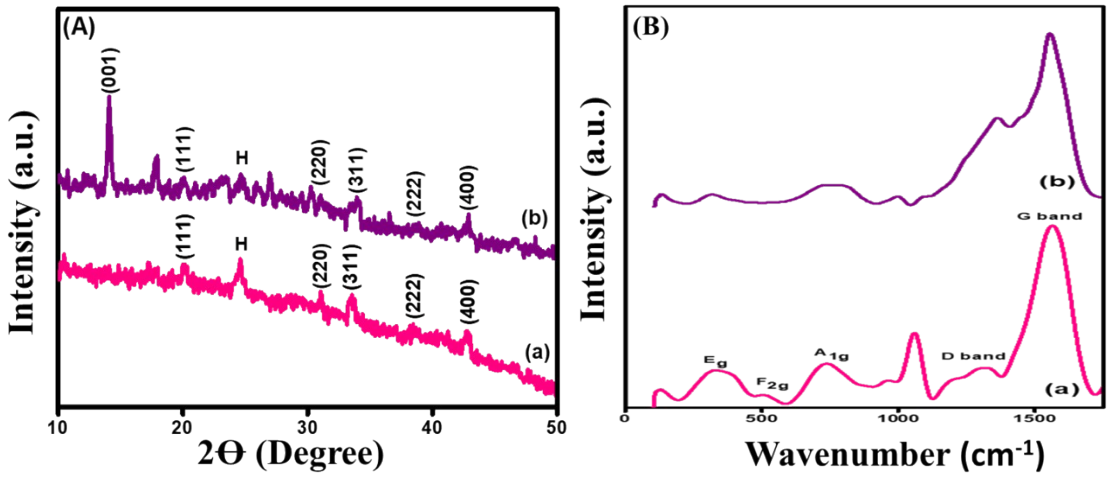

Fig S2. XRD (A) and Raman (B) of (a) Fe_2O_3@Ni (b) Porphyrin/ Fe_2O_3@Ni.

Molecular structure of Porphyrin, Fe_2O_3@Ni and Porphyrin/Fe_2O_3@Ni was also evaluated via FTIR as shown in Fig S3. The peak at 3357 cm^{-1} was accredited to the stretching frequency of N–H group of core porphyrin, and the band between 2840 and 2974 cm^{-1} correspond to stretching of the C–H bond of the aliphatic side chains. A characteristic band at 1658 cm^{-1} was due to the carbonyl stretching frequency. The absorbance band at 1284 cm^{-1} was due to the axial deformation of the C–N bond as revealed in fig S3(a).[1] The band at 650 cm^{-1} was owed to the stretching vibration of (Fe-O) at tetrahedral site which is in good agreement with reported data for nickel ferrite.[2] The lowest band usually witnessed at 400 cm^{-1} exhibit octahedral sites (Ni-O) of nickel ferrite.[3]

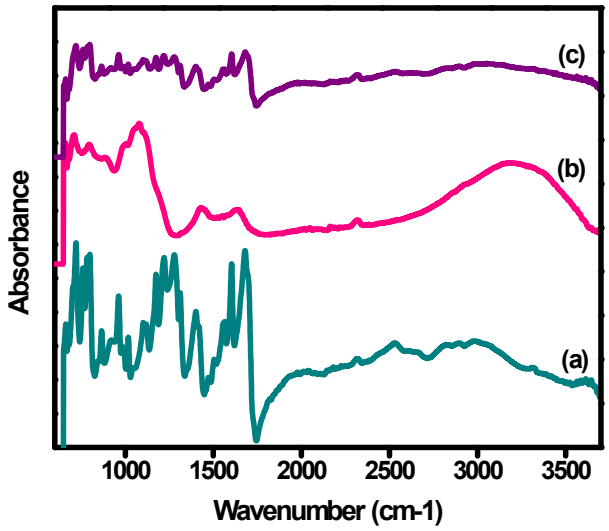

Fig S3. FTIR of (a) Porphyrin (b) Fe_2O_3@Ni (c) Porphyrin/ Fe_2O_3@Ni.

The bands at 1622 cm^{-1} and 3250 cm^{-1} was credited to the bending vibrations and stretching modes of H–O–H or adsorbed water. The band at 1422 cm^{-1} corresponded to the NO stretching vibrations arising from nitrate of residues present in sample as shown in fig S3(b).[4] Meanwhile, the mixed bands were observed in Porphyrin/Fe_2O_3@Ni, depicting the formation of composite due to π-π interactions between these pristine materials as shown in fig S3(c).

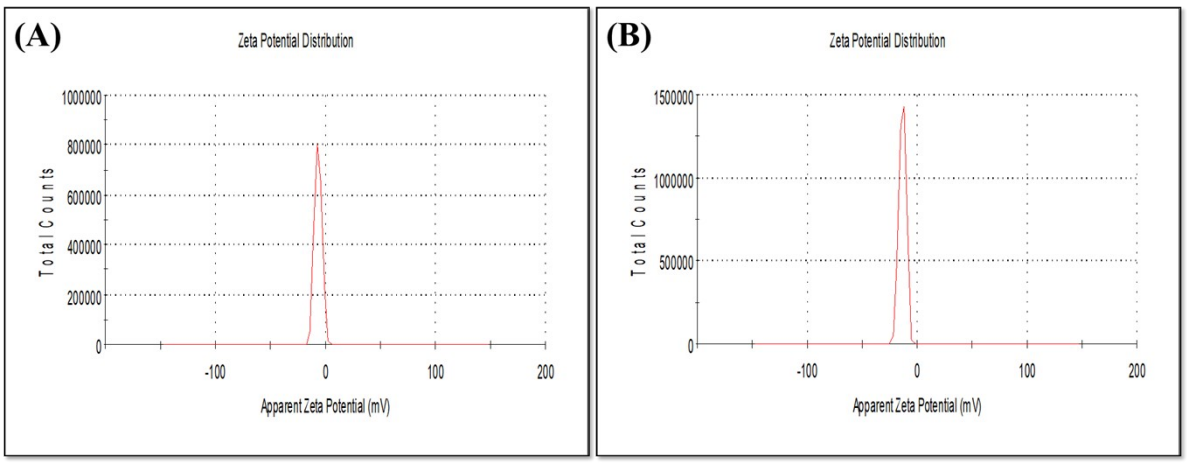

Fig S4. Zeta potential of (A) Fe_2O_3 and (B) Fe_2O_3@Ni

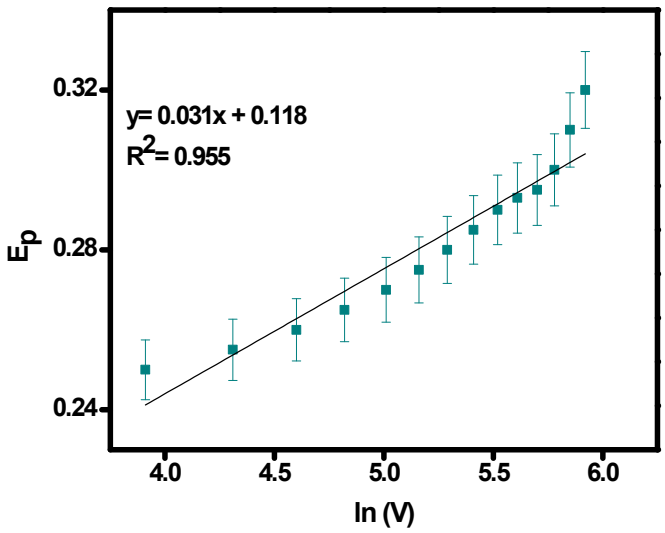

Fig S5.Graph showing relationship among the natural log of scan rate versus peak potential.

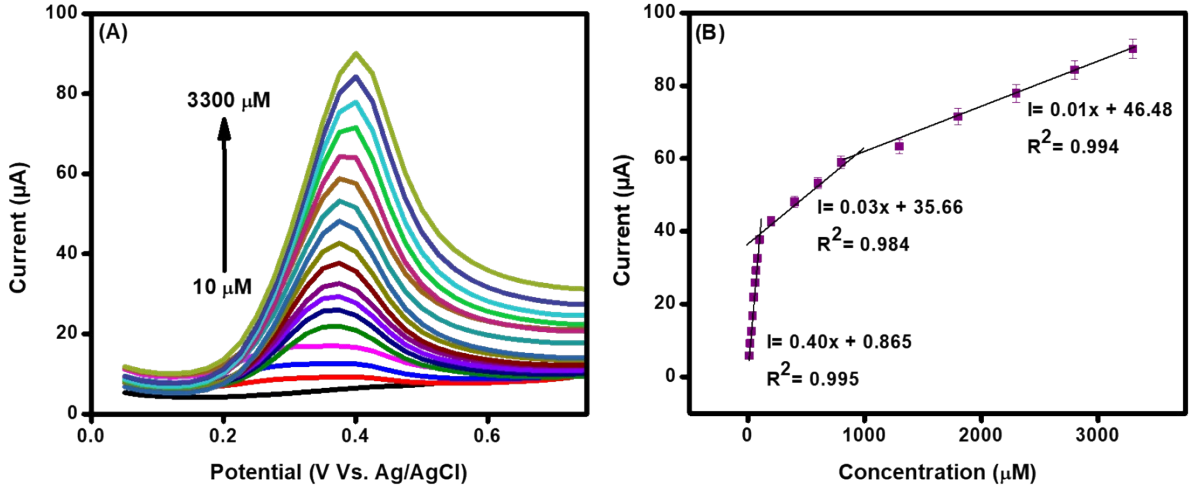

Fig S6. Diffraction Pulse Voltammetry (A), corresponding linear graph (B) for Porphyrin/Fe_2O_3@Ni at concentrations bounds of 10 µM to 3300 µM in PBS at a scan rate of 100 mV/s.

Table S1: Comparison of major features of different modified interfaces for dopamine Screening.

Electrode matrix	Sensitivity ($\mu A \mu M^{-1} cm^{-2}$)	LOD (nM)	Linear range (µM)	Reproducibility (RSD %)	Ref.
CuO/CN-5	0.331	60	16-78.7	-	[5]
Sn@rGO/MnO_2	0.092	120	0–50	-	[6]
RuS_2 /GCE	1.8	73.8	10–80	6.4	[7]
N-rGO-180-8/NH_3	1.82	410	0.5–150	6.22	[8]
PPy/graphene	0.36	2300	100-1000	6.10	[9]
PEDOT-LSG	0.220 ± 0.011	330	1–150	2.7	[10]
SiTi/AuNP/CPE	0.074	570	20-180	5.19	[11]
CdSe/CdS MSQDs	-	97	0.5-15	7.2	[12]
PSi/GCE	0.2715	3.2	0.5-333.3	3.7	[13]
GR/Pt/GR/GPE	-	9	0.06-20	-	[14]
Porphyrin/Fe_2O_3@Ni	**2.6**	**40**	10-3300	1.5	**This work**

CuO/CN-5=copper oxide/carbon nitride; Sn= Stannum, MnO_2 = Maganese oxide; rGO= reduced graphene oxide; RuS_2 = ruthenium (IV) disulfide; N-rGOs= N-doped reduced graphene oxides; PPy= Polypyrrole; PEDOT-LSG =poly(3,4-ethylenedioxythiophene) fabrricated laser scribed graphene; Cu=Copper; CuO= Copper oxide, SiTi/AuNP= silica-titania/gold nanoparticles; MSQDs= magic-sized quantum dots; PSi/GCE= Mesoporous silicon/glassy carbon electrode; GR/Pt/GR/GPE = Graphene nanosheet-sandwiched platinum nanoparticles.

Table S2: Recovery data of the designed sensor in tear samples for DA analysis (n= 3).

Sample No.	Added (µM)	Found (µM)	R %
1	40	35	99.8
2	75	72	99.9
3	100	97	99.9
4	500	450	100.1

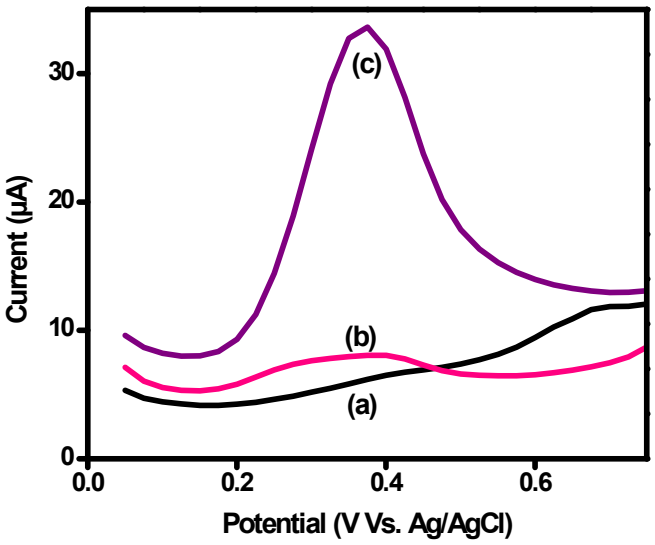

Fig S7. Diffraction Pulse Voltammetry for Porphyrin/Fe_2O_3@Ni in (a) PBS (b) 100 µM of spiked lacrimal fluid (c) after scan and washing with DI water in PBS at a scan rate of 100 mV/s.

References

1. C. Clemente, V. Ribeiro, J. Sousa, F. Maia, A. Barreto, N. Andrade, J. Denardin, G. Mele, L. Carbone and S. Mazzetto, *Journal of nanoparticle research*, 2013, **15**, 1-10.
2. Y. Iqbal, H. Bae, I. Rhee and S. Hong, *Journal of the Korean Physical Society*, 2014, **65**, 1594-1597.
3. J. J. William, I. M. Babu and G. Muralidharan, 2017.
4. B. P. Jacob, A. Kumar, R. Pant, S. Singh and E. Mohammed, *Bulletin of Materials Science*, 2011, **34**, 1345-1350.
5. Y. Huang, Y. Tan, C. Feng, S. Wang, H. Wu and G. Zhang, *Microchimica Acta*, 2019, **186**, 1-9.
6. D. Shanbhag, K. Bindu, A. Aarathy, M. Ramesh, M. Sreejesh and H. Nagaraja, *Materials today energy*, 2017, **4**, 66-74.
7. J. Deepika, R. Sha and S. Badhulika, *Microchimica Acta*, 2019, **186**, 1-10.
8. P. Wiench, Z. González, R. Menéndez, B. Grzyb and G. Gryglewicz, *Sensors and Actuators B: Chemical*, 2018, **257**, 143-153.
9. Z. Rui, W. Huang, Y. Chen, K. Zhang, Y. Cao and J. Tu, *Journal of Applied Polymer Science*, 2017, **134**, 44840.
10. G. Xu, Z. A. Jarjes, V. Desprez, P. A. Kilmartin and J. Travas-Sejdic, *Biosensors and Bioelectronics*, 2018, **107**, 184-191.
11. F. de Matos Morawski, B. B. Xavier, A. H. Virgili, K. dos Santos Caetano, E. W. de Menezes, E. V. Benvenutti, T. M. H. Costa and L. T. Arenas, *Materials Science and Engineering: C*, 2021, **120**, 111646.
12. C. C. L. de França, D. Meneses, A. C. A. Silva, N. O. Dantas, F. C. de Abreu, J. M. Petroni and B. G. Lucca, *Electrochimica Acta*, 2021, **367**, 137486.
13. J. Ahmed, M. Faisal, F. A. Harraz, M. Jalalah and S. Alsareii, *Physica E: Low-dimensional Systems and Nanostructures*, 2022, **135**, 114952.
14. N. Baig, A.-N. Kawde, A. Elgamouz, M. Morsy, A. M. Abdelfattah and R. Othaman, *RSC advances*, 2022, **12**, 2057-2067.